Ninth International Conference on Numerical Ship Hydrodynamics
Ann Arbor, Michigan, August 5–8, 2007

# Resistance Predictions for a High-Speed Sealift Trimaran

K.J. Maki[1], L.J. Doctors[2], S.H. Rhee[3], W.M. Wilson[4], R.F. Beck[1], A.W. Troesch[1]
([1]University of Michigan, [2]The University of New South Wales,
[3]Seoul National University, [4]Naval Surface Warfare Center)

## Abstract

The purpose of this work is to compare the capability of two different numerical techniques for predicting the calm-water resistance of a high-speed sealift trimaran. The vessel is representative of a future advanced naval design that must be able to travel long distances with heavy payloads, but is constrained geometrically in order to operate in austere ports upon arrival. It has a relatively shallow draft and has an extendable centerhull that possesses a wave-piercing bow. This particular design has hulls that are of essentially equal dimensions.

For comparison of the codes, a series of large-scale model tests was conducted for six different configurations of the three hulls (variations of overall vessel beam and length). A thin-ship theory is shown to be effective in predicting resistance. Results for both the absolute value and the relative change in resistance due to change in the hull configuration, together with the computational efficacy of the method demonstrate utility for the designer. The complex effect on the resistance due to the proximity of the three hulls is addressed in a first-principle manner to enhance the prediction from the thin-ship theory.

The commercial computational fluid dynamics code FLUENT is shown to more accurately predict the resistance when the calculations are performed with the body fixed at the experimental sinkage and trim. The temporal expense associated with computational fluid dynamics is reduced in this study by using very simple computational grids. Also, the solution convergence is enhanced by using polyhedral finite volumes which improve cell skewness.

## 1 Introduction

### 1.1 Background

The trimaran vessel has been under consideration for many years now. However, it is only in recent years that the concept has been subjected to high-level technical scrutiny. The reader is referred to books by Dubrovsky and Lyakhovitsky (2001) and Dubrovsky (2004), where the general advantages and disadvantages are explained. Other publications of a design or descriptive nature include those of Summers and Eddison (1995), Pattison and Zhang (1995), van Griethuysen, Bucknall, and Zhang (2001). In these papers, the principal interest has been in the application of the concept to naval vessels, so that the emphasis has been placed on matters of layout and operability, rather than details of resistance and structural strength. The precise categorization of vessel type is often difficult; an interesting example of a hybrid form, namely a small-waterplane-area trimaran, was described by Lamb (2004). A recent example of a successful civil application of the trimaran is that detailed by Armstrong (2004). In the development of that vessel, effort was invested in determining the optimal geometric configuration to minimize both overall resistance and motions in a seaway.

A fundamental question, which must be asked, relates to the potential resistance advantage of a trimaran over more traditional hullforms, such as monohulls and catamarans. Over three decades ago, Narita (1976) examined this problem, using a multibody extension to the hallmark linearized theory of Michell (1898) for a monohull. This matter was also

studied in depth by Doctors (1999), who compared both the wave resistance and the total resistance of vessels possessing between one and six subhulls.

One is strongly interested in minimizing wave resistance if the concern is about the wave generation, such as for river-based ferries, when bank erosion must be avoided. In this case, increasing the number of subhulls is generally favorable, although there is little additional reduction in wave generation after two or three subhulls — depending on the speed range of interest. If there is a primary concern to minimize total resistance, it is found that the increase in wetted surface area is a major drawback of a vessel with many subhulls. Indeed, if a trimaran is to compete on this basis, it is vital to keep to a minimum the size of the sidehulls. In such circumstances, the sidehulls may be referred to as outriggers.

In this current research, we also principally wish to investigate the resistance characteristics of trimarans, because the application is to sealift vessels, in which the operational range is to be maximized. Thus, there is a need to minimize the total resistance. Clearly, the most obvious idea is to consider different longitudinal positions (the stagger) and different lateral positions (the spacing) of the sidehulls. In this regard, one can refer to the work of Wood (1988), Wilson and Hsu (1992), Gale, Hall and Hartley (1996), Ackers, Michael, Tredennick, Landen, Miller III, Sodowsky and Hadler (1997), Battistin, Danielli and Zotti (2000), Doctors and Scrace (2003), Day, Clelland and Nixon (2003), Begovic, Bove, Bruzzone, Caldarella, Cassella, Ferrando, Tincani and Zotti (2005), and Yasukawa (2005). A common theme is that the sidehulls should be located aft in order to reduce the resistance. Obviously, the precise answer must depend on the relative displacements of the centerhull and the sidehull, as well as the intended operational Froude number.

The specific matter of optimization of the configuration of the trimaran is closely linked to the previous comments. This topic has been investigated by a number of researchers, including Suzuki and Ikehata (1993), Yang, Soto, Löhner and Noblesse (2002), Yang, Noblesse and Löhner (2002), Degiuli, Werner and Doliner (2003), and Brizzolara, Bruzzone, and Tincani (2005). When studied in a theoretical or computational sense, it must be understood that the problem is nonlinear. That is, the only reliable approach to determining the global optimum is through a search technique that is coded in order to avoid local false optimums.

It is necessary to test theoretical prediction methods against experiments. This is most conveniently achieved at model scale in a towing tank. Examples of such effort is characterized by the papers by Scrace (2000), Kennell (2004), Mizine, Amromin, Crook, Day and Korpus (2004), Colicchio, Colagrossi, Lugni and Faltinsen (2005), and Degiuli, Werner and Zotti (2005). In general, it can be stated that current methods based on the Michell (1898) theory or computational fluid dynamics (CFD) provide useful results. Nevertheless, the predictions are often not as accurate as those for catamarans. It is believed that this is due to the possible strong flow interferences between the sidehulls and the centerhull, which can create an adverse effect (that is, a large increase) on the frictional form factor. We will specifically refer to this point again later in this paper.

## 1.2 Current Work

In the current work, we describe an exhaustive investigation into the resistance for a candidate high-speed sealift trimaran. The purpose of the effort was twofold: to consider a suitable trimaran design and to test our available computational tools.

The software developed by Doctors (1999) and Doctors and Scrace (2003), based on extensions to the Michell (1898) theory, represented one focus of the computational work. Computations were performed in a "blind fashion", in that the experimental results for the resistance were not initially made available to those persons performing the calculations. Of course, the opportunity was later provided to learn from the comparisons of theory and experiment and, consequently, to improve the software.

The second focus of the work was based on a Reynolds-Averaged Navier-Stokes (RANS) computational fluid dynamics (CFD) approach using the commercially available software FLUENT. The initial intentions were to perform the computations in a "blind fashion", as in the Doctors results; however, difficulties were encountered in dynamically predicting the sinkage and trim of the model as part of the computations. Therefore, several fixed model conditions were simulated, using the experimentally measured sinkage and trim for the model. It is not

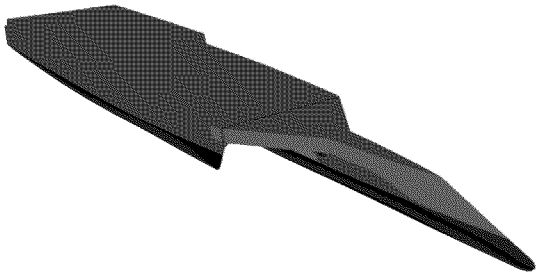

(a) Pictorial of Configuration 6

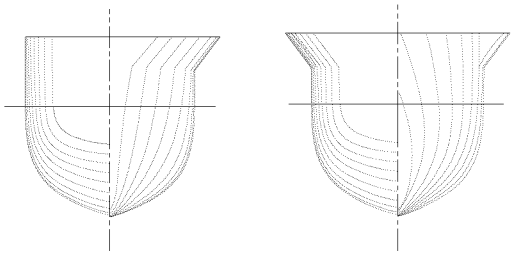

(b) Side Hull (c) Center Hull

Figure 1: Vessel Geometry

yet clear what the limiting factor is for predicting the sinkage and trim of the model. Previous investigations by some of the authors have successfully computed ship model behaviors for pitch and heave in the presence of incident waves (Sasanapuri, Shirodkar, Wilson, Kadam, and Rhee, 2007), and further studies are planned to include the dynamic motion of the model as part of the computations.

# 2 Design of Candidate

## 2.1 Geometry

The vessel chosen for our investigation is a trimaran, in which the sidehulls and the centerhull are essentially equal in length, beam, draft, and displacement. The vessel is depicted in Figure 1, where the perspective view of the extended vessel can be seen along with the body plans of the side and center hulls.

Both the centerhull and the sidehulls possess a transom stern, which would permit the installation of suitable waterjets. The principal geometric and hydrostatic data for the subhulls are listed in Table 1, for the loading cases where the draft is set at 6.510 m.

## 2.2 Advantages of Concept

It is well known that a resistance-optimal conventional trimaran is one in which the sidehulls possess a very small displacement compared to that of the centerhull. However, in the present application, it is intended that the trimaran will be operated in essentially two different (and diverse) modes.

In the cruising mode, the sidehulls are to be staggered rearward by up to 50% of the length of the subhulls. In this configuration, the great overall length of the vessel renders it somewhat similar to a slender monohull from a resistance point of view. Thus, its resistance qualities are expected to be good. In the arrival or departure mode, the centerhull can be retracted so that it is aligned with the sidehulls. While the resistance is certain to be unreasonably high in this configuration, it will permit the vessel to be docked in an austere port.

This vessel was designed by Dr R. Scher, of Alion Science and Technology, in Alexandria, Virginia. The designing of this vessel formed part of the project *Architectural Concepts and Hydrodynamic Technologies for High Speed Sealift to Austere Ports: Subtopic B: Computational Approach and Hydrodynamic Tools*, supported by the US Office of Naval Research, under the supervision of Project Manager Dr. L. Patrick Purtell.

# 3 Towing-Tank Tests

## 3.1 Physical Description of Model

The bare-hull model resistance tests were conducted at the Maritime Research Institute Netherlands—MARIN. Three individual hulls were constructed out of wood, with a scale factor of 1:34, and connected together using aluminum beams which allowed for easy reconfiguration. Figure 2 shows an image of the model in Configuration 4.

The model was attached to the carriage and towed with a vertical heave staff and gimbal so that the model was free to heave and pitch. The longi-

Table 1: Nominal Particulars of HSSL ALT Subhulls

| Item | Symbol | Units | Center-hull | Side-hull |
|---|---|---|---|---|
| Displacement mass | $\Delta$ | t | 5827 | 5964 |
| Waterline length | $L$ | m | 168.1 | 168.6 |
| Waterline beam | $B$ | m | 10.03 | 10.04 |
| Draft | $T$ | m | 6.510 | 6.510 |
| Waterplane-area coefficient | $C_{WP}$ | | 0.7770 | 0.8091 |
| Maximum section coefficient | $C_M$ | | 0.7860 | 0.7863 |
| Block coefficient | $C_B$ | | 0.5174 | 0.5279 |
| Prismatic coefficient | $C_P$ | | 0.6583 | 0.6714 |
| Slenderness coefficient | $L/\nabla^{1/3}$ | | 9.424 | 9.375 |

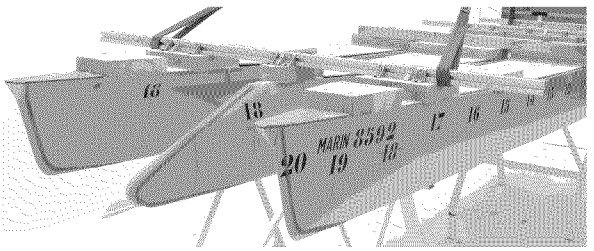


Figure 2: Image of model in Configuration 4

tudinal location of the tow point corresponded to the longitudinal center of buoyancy of the trimaran (which varied depending on the stagger of the sidehulls).

## 3.2 Test Configurations

The towing-tank model was operated in six different loading configurations, as listed in Table 2 and viewed in Figure 3. Essentially, this consisted of three different staggers of the sidehulls and two different offsets $s_2/2$ of the centerplane of the sidehulls from the centerplane of the centerhull. During the planning phase of the experiments, we had intended that the draft should be identical for all test configurations. Unfortunately, the freeboard proved to be too small for the reduced dimensions for Configuration 4 and Configuration 5; as a result, an excessive amount of spray impacted on the bridging cross structure connecting the three subhulls. This deficiency in the design of the trimaran could easily be corrected in any planned extension to the project.

It is recommended that the wetdeck height, which in the current design is 10.63 m, be increased

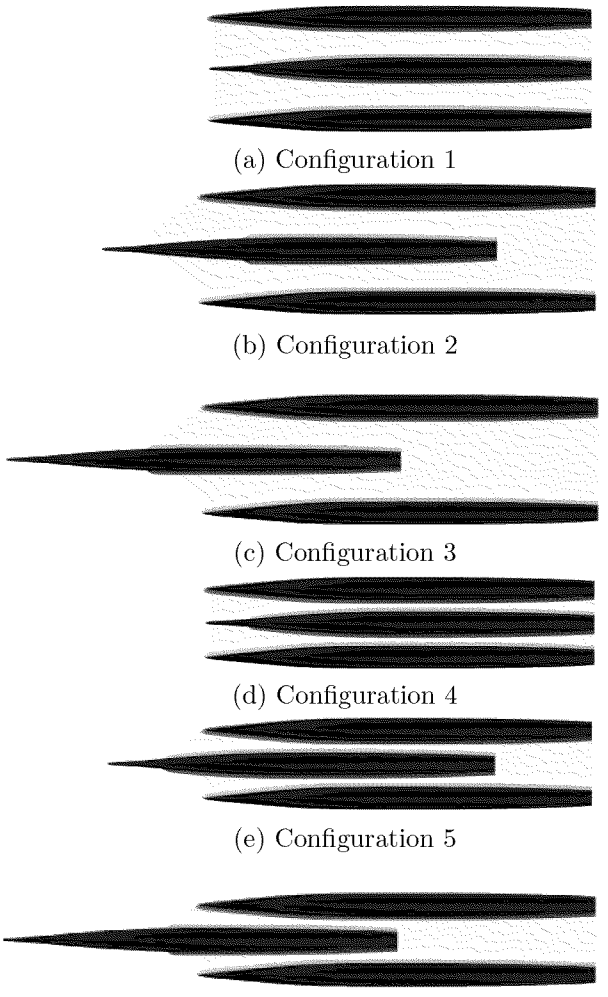

(a) Configuration 1

(b) Configuration 2

(c) Configuration 3

(d) Configuration 4

(e) Configuration 5

(f) Configuration 6

Figure 3: Bottom View of the 6 Hull Configurations

by a minimum of 2 m. This is based on observations of the resistance tests and of the seakeeping experiments that were performed on the model. (Seakeeping experiments were also done solely for Configuration 6 and the model was self-propelled with a single water jet fitted in each hull.) Two factors contributed to the relative rise of the free surface on body. Firstly, the geometry of the shorter Configurations 1, 2, 4 and 5 places the forward portion of the sidehulls in the peak of the dominant-diverging wave of the centerhull. Secondly, the vessel sinks downward and trims bow down at a speed of approximately 30 knots. Figures 4 and 5 depict the effect of forward speed on the running attitude of the body, and thus the freeboard. Figure 4 shows in the deep draft Configuration 4 at 30 knots, and the vanishing freeboard can be seen. Note that the models were tested with the portion of the geometry from the baseline to the wetdeck plane. Figure 5 shows how the vessel attitude changes at a higher speed. The bow-up trim and rise in the vessel act to increase the freeboard on the vessel.

Other observations from the seakeeping experiments suggest that a 2 m rise in the wetdeck should be sufficient to allow clearance for the spray and jet of water exiting the centerhull. Finally, a rise in the wetdeck will allow for larger free-board on the centerhull, which is currently limited by the fact that it must retract underneath the sidehulls for entry into *Port Austere*.

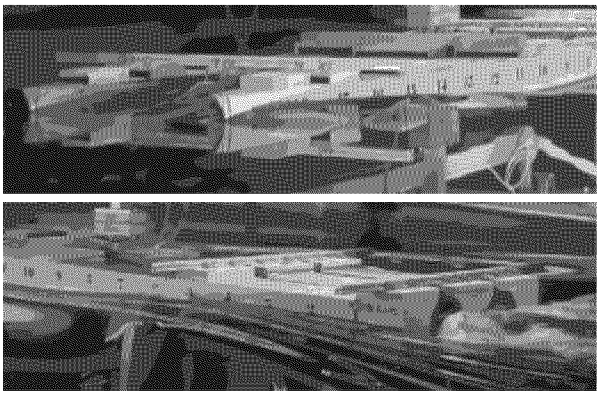

Figure 4: Image of model underway, in the *heavy* Configuration 4 (ballasted to a draft of 6.51 m), at a speed of 30 knots

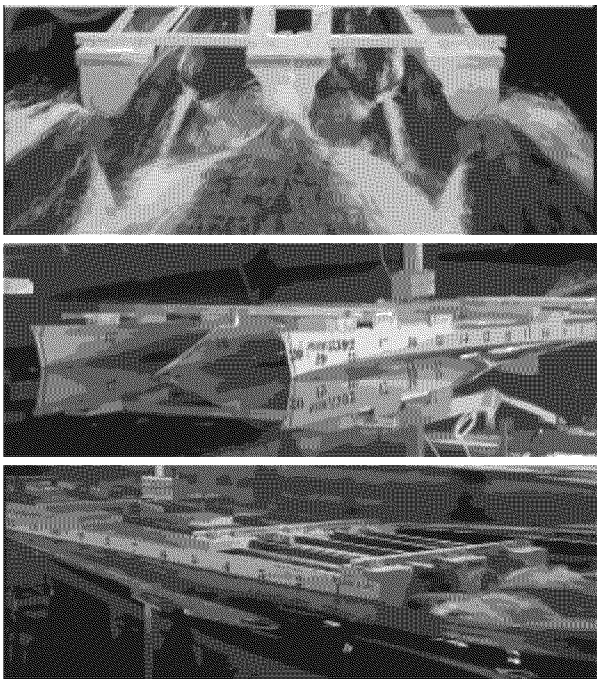

Figure 5: Image of model underway, in Configuration 1, at a speed of 44 knots

# 4 Theoretical Approach

## 4.1 Thin-Ship Analysis of a Transom-Stern Multihull

A computational approach based on the work of Doctors and Day (1997) was used to predict the resistance of the 1/34-scale model. This approach has its roots in the linearized theory of Michell (1898). The current version of the software contains a number of enhancements.

Firstly, the program can handle any number of subhulls up to six, by employing additional centerplane source distributions. The transverse velocities induced by one subhull should be corrected for by the use of centerplane dipole distributions; however, this is ignored for the sake of considerable simplification to the coding of the software.

Secondly, an enhanced model for the transom-stern flow has been under development for ten years now. The current model allows for a realistic hydrodynamic addition to the vessel by means of a virtual extension to the vessel in order to represent the presence of the transom-stern hollow. This has

been described by Doctors and Beck (2005), Doctors (2006a and 2006b), and Maki, Doctors, Beck, and Troesch (2006). In this way, the effective hydrodynamic length of the subhulls grows with increasing vessel speed in a physically realistic manner that has been substantiated by numerous towing-tank experiments.

Thirdly, the transom-stern model includes a procedure for estimating the progressive unwetting or ventilation of the transom. This feature permits a practical estimate of the transom-stern or hydrostatic drag suffered by such vessels.

Fourthly, as a special task inspired by the model experiments to be described here, a further procedure was incorporated in the computer code in order to take into account the viscous interaction between the subhulls. This simplistic procedure makes an allowance that the subhulls are in the "shadow" of each other to some degree, as seen in a profile or a side view. This shadow will be greatest when the subhulls are abreast of each other and will be particularly strong when they are of similar size. In the present theory, the local gap between the subhulls below the loaded waterplane was computed. From this, an estimate of the increase in local water speed was obtained. This increase in speed was applied to the usual formula for frictional resistance, thus leading to an approximate technique for determining the frictional form factor.

Of course, it is clearly understood that a number of physical phenomena is neglected here. Neglected effects include the deformed shape of the free surface and the fact that the flow would tend to skirt around the outside of the vessel in cases where the intersubhull gap is very small. However, we wished to preserve the characteristically simple approach of the software as well as its fast computational behavior.

## 4.2 Analysis Using RANS

Computational fluid dynamics codes have demonstrated increasing fidelity in recent years in predicting the Kelvin wave structure for a variety of ships and marine craft. Advancements in computational methods for free-surface predictions using level-set and volume-of-fluid (VOF) techniques have demonstrated marked improvements in the ability to accurately predict flows around surface ships that are moving at speeds that cause breaking waves. Recent advances in computing technologies and, in particular, parallel-processing techniques, have also greatly enhanced the ability to perform simulations with increased spatial resolution of the flow field and with faster compute times. These improvements, along with growing user experience in applying RANS methods to these types of problems, are beginning to demonstrate the ability of CFD methods to impact design and evaluation for marine hydrodynamic problems. A review of applying RANS techniques to a variety of surface ship configurations was given by Gorski (2004). An assessment of different computational tools was given in Wilson, Fu, Fullerton, and Gorski (2006).

The commercially available viscous RANS flow solver FLUENT was used to predict the resistance for the 1:34-scale model. The computations focused on Configuration 6 (Figure 3(f)) as this was expected to be the best performing design configuration for resistance and seakeeping. The computations were performed using FLUENT V6.3 and the parallel computational resources at the Ship Engineering and Analysis Technology Center, located at the Naval Surface Warfare Center, Carderock Division (NSWCCD) and the Aeronautical Systems Center (ASC) Major Shared Resource Center (MSRC) High Performance Computing facility.

The CFD software uses a cell-centered finite-volume method and allows a variety of different computational element (cell) types, including quadrilateral, tetrahedral, hexahedral, pyramidal, prismatic, and hybrid meshes. The latest version of the software also includes the ability to convert tetrahedral mesh zones into polyhedra, which are constructed from an arbitrary number of sides. Computational meshes constructed from polyhedra have several advantages, including reduced computational cell count and greatly improved mesh quality through reduced cell skewness. Both of these attributes have a significant positive effect on solution convergence.

The computational grids for performing the CFD calculations employed hexahedral volumes in the far-field, boundary-layer prisms on the hulls, and polyhedral volumes to connect the boundary-layer prism caps to the far-field volume. This decomposition exploits the advantages of each of the different types of finite-volume cell, while also considering the desire to minimize the difficulty in grid generation.

Table 2: Details of Model Experiments

| Configuration | Overall Length $L$ (m) | Overall Beam $B$ (m) | Sidehull Stagger $r_2$ (m) | Sidehull Offset $s_2/2$ (m) | Draft $T$ (m) | Displacement $\Delta$ (t) | Speed Range $U$ (kn) |
|---|---|---|---|---|---|---|---|
| 1 | 168.6 | 56.0 | 0.0 | 23.0 | 6.51 | 17,756 | 20–56 |
| 2 | 210.6 | 56.0 | −42.5 | 23.0 | 6.51 | 17,756 | 20–60 |
| 3 | 253.1 | 56.0 | −85.0 | 23.0 | 6.51 | 17,756 | 20–54 |
| 4 | 168.2 | 39.9 | 0.0 | 15.0 | 5.19 | 12,341 | 20–54 |
| 5 | 210.2 | 39.9 | −42.5 | 15.0 | 5.19 | 12,341 | 20–48 |
| 6 | 253.1 | 40.0 | −85.0 | 15.0 | 6.51 | 17,756 | 20–58 |

Figure 6 shows the surface mesh on the centerhull and centerplane where each of the three different cell types can be seen. Also visible in this Figure is the thickness over which the free surface is artificially spread due to numerical discretization. The thickness is seen to be at most three cells, a value that it not intolerable because even the most advanced and thus complex advection schemes rarely compress the interface to fewer than two cells.

The hexahedral volumes are effective in solving both the undisturbed free-surface upstream of the body and the diffracted waves away from the body, with a minimum number of finite volumes. This is contrary to the polyhedra which are better suited for filling volumes of the flow domain that are defined by complex geometry but compromise interface resolution.

The polyhedra are touted to reduce the cell count by up to a factor of five when compared to a tetrahedral unstructured grid, but such a large reduction of unknowns must have an impact on the resolution of the flow field. In this application, the polyhedra were created from a tetrahedral mesh, and as to not excessively reduce the resolution by losing too many cells, the original tetrahedral mesh was created with a much greater density.

The division of two separate domains permits that one far-field grid be generated and used for all calculations and a new inner domain be generated for each simulation that requires the hull be arranged with a different sinkage and trim. The outer domain had extents of $(x, y, z) \in (-20.0, 0.0, -20.5) : (40.0, 20.0, 20.5)$ in model scale units of meter. The inner domain extended from $(x, y, z) \in (-8.0, 0.0, -0.5) : (1.0, .75, 0.5)$. The Cartesian coordinate system is situated at the centerline, transom, calmwater intersection, and oriented with $z$ vertically upwards and $x$ downstream. A layer of boundary-layer prisms was generated on each hull. The first cell had a height of 0.001 m and at the speed of 40 kn this resulted in wall $y^+$ values between 2.0 and 100, with the average value of 39. The grids used in this work had a total cell count of approximately 1.6M, composed of 1.34M polyhedra and 265K hexahedra.

In the present study, the convective terms were discretized using the QUICK scheme (Leonard, 1979). This scheme uses a weighted average of upwind and central second-order interpolation methods, which is typically more accurate for structured grids aligned with the flow direction. For unstructured meshes, the scheme reverts to the second-order upwind method. Therefore, this scheme is very appropriate for the present case, which involves a hybrid mesh that contains both structured hexahedral elements which are mostly aligned with the general flow direction, as well as polyhedra elements for flexibility in resolving the model geometry and near-body flow. The discretization of the volume fraction equation used a modified version of the high-resolution interface capturing (HRIC) method (Muzaferija, Peric, Sames, and Schellin, 1998). The HRIC scheme has been shown to be more accurate than the QUICK or other second-order discretization schemes, and is less computationally expensive than using a complete geometric reconstruction of the interface. The turbulence closure was accomplished using a model that is a variant of the $k - \omega$ model as described in Wilcox (1998).

The simulations were performed as fully unsteady in time, marching to an equilibrium solution. The time advancement was accomplished using second-order backward differencing, and algebraic multi-grid methods were used to aid in the solution convergence.

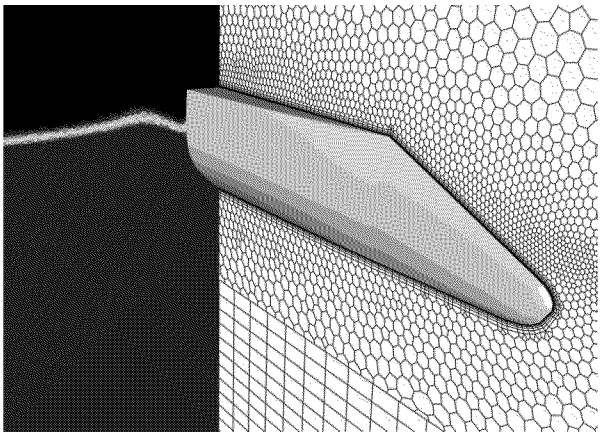

(a)

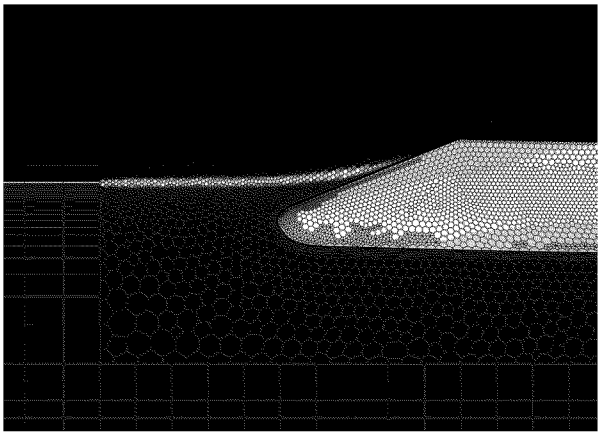

(b)

Figure 6: CFD grid and flow solution. Contours of volume fraction depict the location of the free-surface for the 40 knot speed case

# 5 Results

## 5.1 Comparison of Theory and Experiment

We turn to Figure 7, whose six parts show the experimental and computed results for the abovementioned six configurations. The symbols on these plots are listed in Table 3.

The curves for the resistance components are all represented in a dimensionless form known as the *specific resistance*, namely, the ratio of the resistance to the vessel weight. It is important to clarify that the calculations are all executed at model scale in order to be directly comparable with the model experiments. However, the results are plotted with the velocity expanded to full scale using Froude scaling.

Table 3: Nomenclature

| Symbol | Meaning |
|---|---|
| $U$ | Speed of vessel |
| $W$ | Displacement weight |
| $f_s$ | Surface-velocity limit factor |
| $r_2$ | Stagger of sidehull |
| $s_2/2$ | Offset of sidehull |
| $\Delta$ | Displacement mass |
| $R_F$ | Frictional resistance |
| $R_H$ | Hydrostatic resistance |
| $R_T$ | Total resistance |
| $R_W$ | Wave resistance |
| $R_{\text{air}}$ | Air resistance |

We first consider Configuration 1 in Figure 7(a). The wave resistance $R_W$ possesses its typical maximum at the "hump" condition. The hydrostatic resistance $R_H$ is seen to be relatively small, indicating that little of the transom is immersed in the water. The frictional resistance $R_F$ is estimated from the 1957 ITTC line and is seen to be the major drag component at the high-speed end of the speed range, namely at 50 to 60 knots. The simple sum of these components is indicated by the first of the curves for total resistance $R_T$. This predicted result may be compared with the experimental data as represented by the symbols.

It can be seen that this first prediction of the total resistance, indicated by the symbol $f_s = 1$, falls short of the experimental resistance. This discrepancy increases with speed. It is believed that most of this discrepancy can be traced back to the interactions between the subhulls increasing the frictional drag, as noted earlier in this paper.

To emphasize this point, one has only to note that the subhulls each possess a maximum local beam of approximately 10 m at the waterline. With an overall sidehull-centerplane spacing $s_2$ of 46 m, this leads to a minimum gap of 13 m. This suggests that the water has been channeled from an initial width of 23 m down to 13 m, implying a large increase in the local speed of the water over the surface of the hull. On the other hand, it should be noted that this effect will be much less on other parts of the subhull surface. The current estimate of the velocity increase does take this effect fully

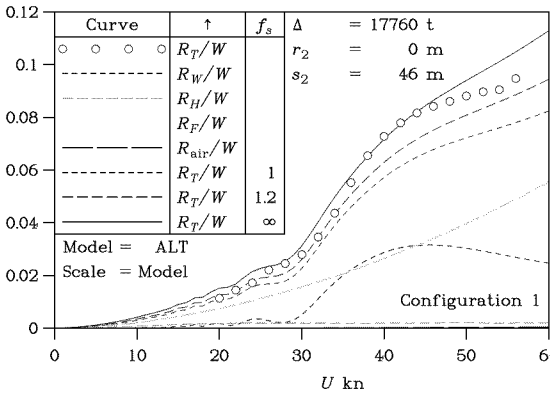


(a) $L = 168.6$ m, $B = 56.0$ m

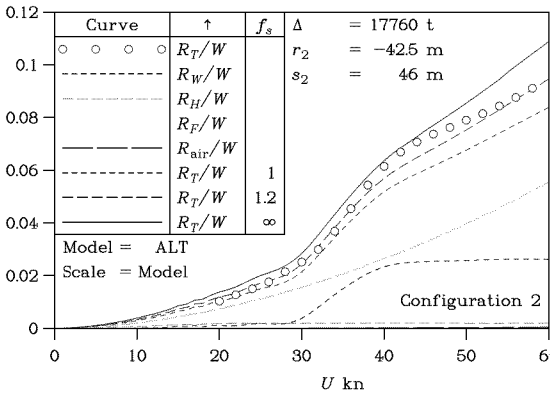


(b) $L = 210.6$ m, $B = 56.0$ m

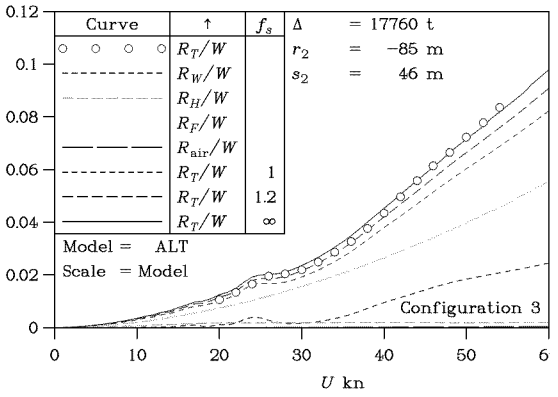


(c) $L = 253.1$ m, $B = 56.0$ m

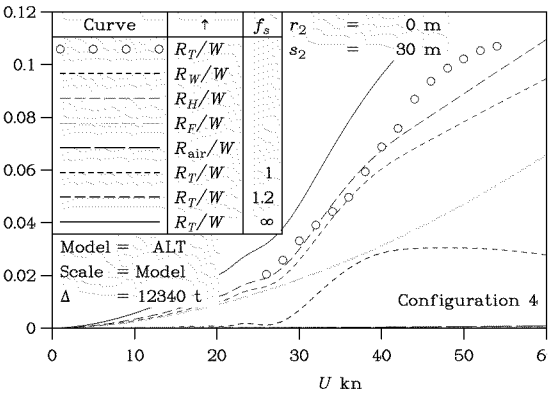


(d) $L = 168.2$ m, $B = 39.9$ m

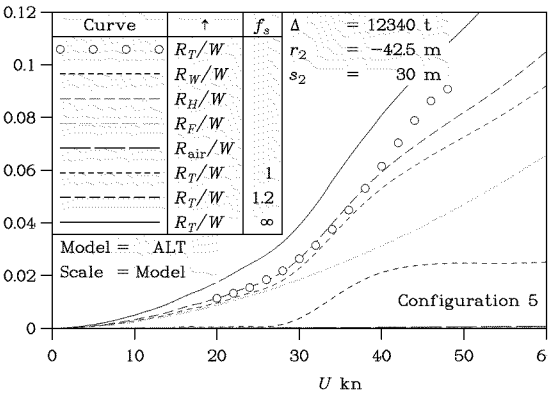


(e) $L = 210.2$ m, $B = 39.9$ m

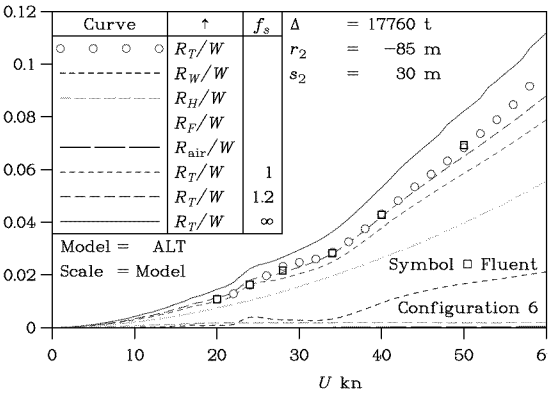


(f) $L = 253.1$ m, $B = 40.0$ m

Figure 7: Components of Resistance at Model Scale. (○) experiment; (−) thin-ship theory; (□) FLUENT

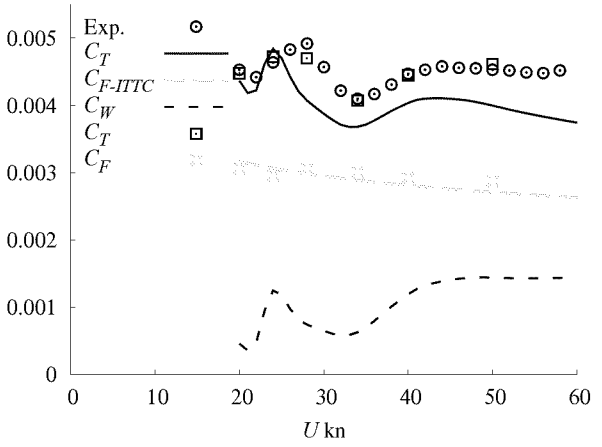


Figure 8: Resistance coefficients at model scale, Configuration 6. (○) experiment; (−) thin-ship theory with no form factor; (□) FLUENT

into account in the third theoretical prediction, indicated by $f_s = \infty$.

It is considered that the prescription explained here overestimates the effect under study, as noted when the vessel speed $U$ exceeds 44 knots. Thus, yet another curve is shown, indicated by $f_s = 1.2$. The meaning of this is that the coding places an upper limit on the subhull surface velocity of 1.2 times the vessel speed.

The other five parts of Figure 7 pertain to the other five configurations. On the whole, it is confirmed that the surface-velocity limit factor $f_s = 1.2$ does seem to be a reasonable compromise for achieving the best correlation between theory and experiment.

Figure 7(f) also shows some calculations based on the FLUENT software. Because computational times are much greater for these very extensive and detailed CFD studies, a limited number of computed points only is depicted here. It is indeed most encouraging to observe the excellent matching between the FLUENT data points and the experimental data.

Figure 8 contains the data of Figure 7(f) replotted non-dimensionally as the resistance coefficient, $C_T = R_T/(1/2\rho U^2 S)$, at model scale. Thus, there is no scaling included in the experimental result. The thin-ship theory results are calculated with the surface-velocity limit factor $f_s = 1.0$. That is, a frictional form factor of 1.0 is employed here. Clearly, the use a larger value of the form factor, such as $1 + k = 1.20$, would provide excellent predictions for the thin-ship theory code. The results show good agreement by both codes with the experimental data, but more accurate results are provided by the FLUENT RANS code. The average relative difference between prediction and experiment, when using the speed range of 20 to 50 knots, is 9.9% and 1.8% for the thin-ship theory and CFD results respectively. When comparing the two computational methods, we must recall the extra expense of the increased accuracy. The time required to complete a converged drag result for a single forward speed is approximately 24 to 48 hours using 24 processors for the RANS method and only about 1 second on a single processor for the thin-ship theory code.

A sample prediction of free-surface elevation from the RANS computations for an equivalent forward speed of 40 knots is shown in Figures 9. Interrogation of the three-dimensional flow solution is very useful in understanding the resulting Kelvin wake pattern, as well as the stern wake flows and the interference effects between the center and side hulls. A closer examination of these figures also points out how the solution of the wave profiles becomes somewhat degraded as the flow information is transmitted across the non-conformal grid interface separating the near-body region from the outer domain. Because the focus of this effort was to examine the ability of the tools to predict the model resistance, this was deemed an acceptable way to relax the mesh resolution requirements, while not significantly impacting the resistance computation, as evidenced by the results in Figures 7(f) and 8. Of course, if one were interested in accurately predicting the wave behavior further away from the hull, then commensurate mesh resolution would be required. Wilson, Fu, Fullerton, and Gorski (2006) have shown that increased grid resolution enables a more accurate prediction of the wave elevation, but the effect on resistance prediction is still unclear.

It is also conjectured that there is perhaps a fundamental physical effect of the sidehull wave interference drag which is being better represented by the RANS method. The sidehull wave interference effect can be seen in Figure 10. As pointed out earlier, this effect increases with increasing forward speed; hence, the discrepancy between the two computational methods grows larger at the higher speed range. We restate that the RANS simulations are conducted without including the sinkage and trim

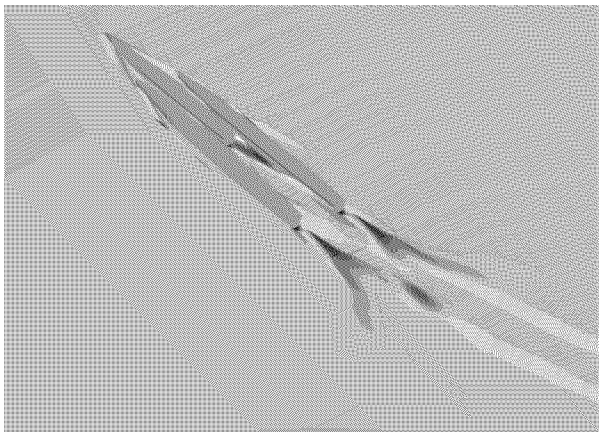

(a)

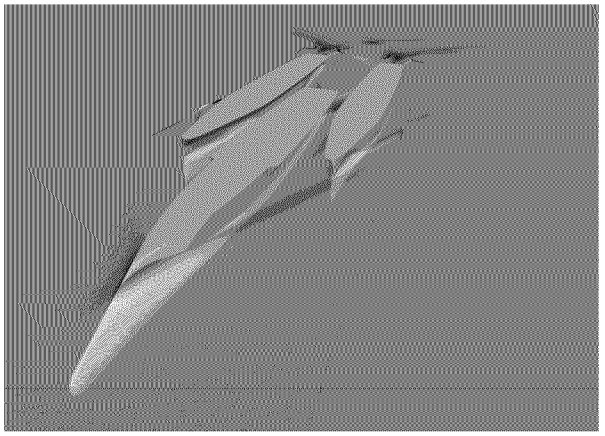

(b)

Figure 9: Free-surface contours colored by elevation

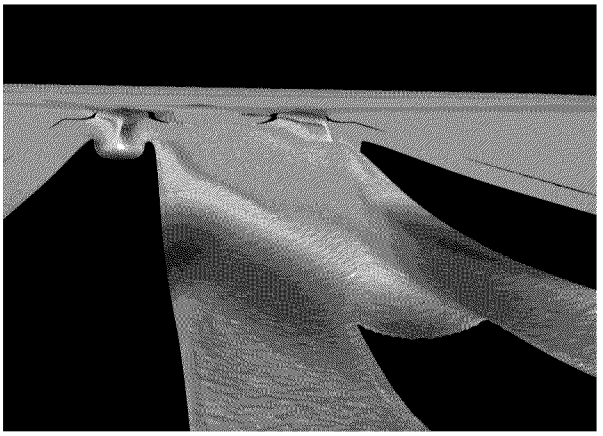

Figure 10: Contours of free-surface elevation mapped onto the the free surface. Camera is located between the center and starboard hulls, looking aft

prediction as part of the computation, but rather the model attitude is fixed based on the experimentally measured sinkage and trim. This most likely provides a reduction in the error by eliminating the difference between the predicted and physical model sinkage and trim that would propagate into errors in the predicted hull forces.

## 5.2 Effect of Changes to Configuration

We now proceed to Figure 11, in which we compare the change in total resistance when comparing two different configurations.

Figure 11(a) shows the fractional change in specific total resistance $\Delta R_T/W$ between Configuration 1 and either Configuration 2 or Configuration 3. We can point out two important features. Firstly, the experiments indicate a reduction in specific total resistance of 0.029 for the greater sidehull stagger of $-85$ m at a speed of 40 knots. This represents an impressive saving and it vindicates the unusual and novel nature of our trimaran concept.

This reduction in total resistance would be different at prototype scale because of the difference in the Reynolds number.

Secondly, it is heartening to note that the theory predicts the nature of the resistance reduction observed in the experiments. However, at the design speed of 40 knots, the prediction suggests a reduction of only 0.021.

Finally we turn to Figure 11(b), which is a plot of the *ratio of the two resistances* $\Delta R_T/R_T$, rather than a difference which was plotted in Figure 11(a). With this form of plot, the relative overall agreement between theoretical predictions and experiments is actually more encouraging. From a practical viewpoint, we see that there can be a relative reduction in total resistance of up to 43%, at a speed of 38 knots.

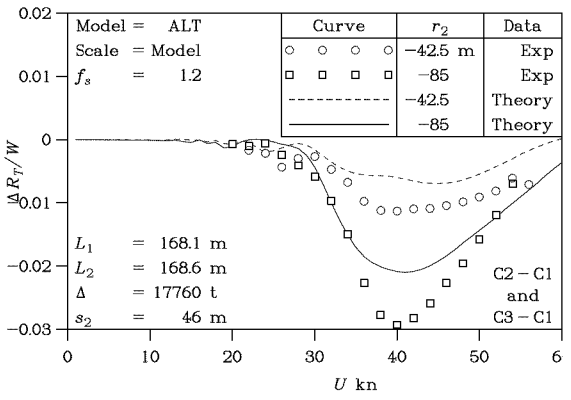


(a) Difference in change in configuration

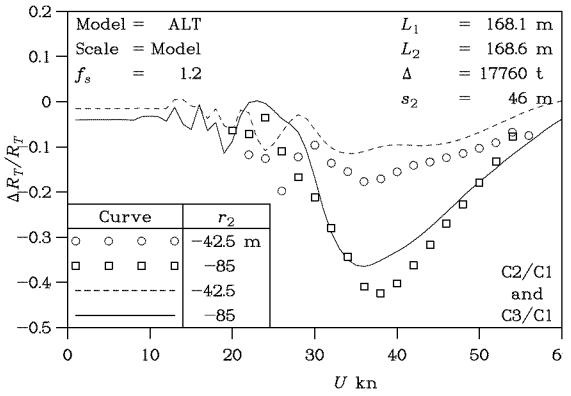


(b) Ratio of change in configuration

Figure 11: Change in resistance: Configuration 2 and Configuration 3 WRT Configuration 1

# 6 Conclusions

## 6.1 Current Work

This paper contains the results of calm-water resistance prediction for a high-speed sealift trimaran. The two numerical codes that were used are a thin-ship theory and the commercial CFD software FLUENT.

It has been demonstrated that the thin-ship approach, as exemplified by the results plotted in Figure 7, Figure 8, and Figure 11, provide remarkably reasonable estimates of the total resistance, if one simply adds the theoretical wave resistance $R_W$, the hydrostatic drag $R_H$, and the ITTC 1957 frictional resistance $R_F$. It should be borne in mind that computational times are typically one second per speed, using a computational grid of 60 panels longitudinally and 20 panels vertically. Thus, the CPU time is six of seven orders of magnitude less than that required for the CFD computations. Of course, the CFD results are considerably more useful, because they provide data for the complete flow field and would be beneficial to the naval architect in many ways.

Figure 7 has been used to demonstrate the effectiveness of employing a frictional form factor $f_F = 1 + k$, which has been calculated through an estimate of the increased subhull surface velocities due to the subhull-proximity effects, as already detailed. The method developed so far results in a value of $f_F \approx 1.20$. That is, it is suggested that the frictional resistance in such cases of closely spaced subhulls is increased by about by 20%. The use of such a factor in Figure 8 would bring the thin-ship predictions into nearly perfect alignment with the full CFD computations, without the need for any significant additional CPU time.

The CFD results contained in this paper were calculated with a rudimentary grid generation approach that reduces set-up and solution time. A goal of the project which supported this work was to evaluate the codes for transfer to a shipyard and/or design office. Often in the application of CFD, the grid generation is a frustrating hurdle for users to overcome, so the approach here is very simple to effect, yet it does not seem to sacrifice accuracy. The overall domain is divided into near-field and far-field regions that are filled with polyhedral and hexahedral cells respectively.

The polyhedral finite-volume cell that was used drastically reduces cell skewness and overall cell count. The reduced skewness causes the equation coefficient matrices to be more diagonally dominant, and thus improves solution convergence and robustness.

The accuracy of the CFD results was outstanding. The error relative to the experimental values was on average less than 2% with a maximum of 4%. We remind the reader that the CFD predictions are done using the experimental values of sinkage and trim.

The reconfigurable catamaran is shown to dramatically reduce its total drag by extending the centerhull. The experiments dictate a 43% reduction in total drag at model scale. This reduction is sufficient to encourage further investigation of the con-

cept, namely consideration of the actuation system for the extending hull and requisite gear, and the impact on the hydrodynamic performance. Also, during the initial design period, it was unclear which sidehull spacing would be best for low resistance. Interestingly, it was the narrowest Configuration 6 that had the lowest drag, though the effect was very small.

### 6.2 Future Work

The authors are encouraged by the quality of the results from both the thin-ship theory and CFD. At the same time, there are issues which will be valuable to investigate further to expand the utility of these numerical tools for the designer.

The thin-ship predictions can be improved by a more careful study of the frictional form factor, which is thought to be the main cause of the total drag estimate being a little low. The reader is reminded that, in the literature, there is a large body of evidence indicating that for some vessels, the frictional form factor might be as high as 1.40 — far exceeding the model value of around 1.20 indicated earlier.

Another point is the estimate of the length of the hollow, which is assumed to grow as the speed increases, following the extensive model tests reported by Doctors (2006a and 2006b). This increase in effective hydrodynamic length of the vessel lowers the predicted wave resistance. Studies of this matter are also in the planning stage.

The CFD calculations are very expensive in both the need of parallel computational hardware and the long computational time to arrive at the converged solution. Any research that aims at rendering the solution algorithms more efficient, or reducing the number of unknowns would be valuable. It is natural to expect the solution quality to improve with increased grid density, though this has not been proven unequivocally for CFD surface-ship resistance predictions. With the new polyhedra element now emerging in the CFD community, and the always evolving naval combatant hull forms, a detailed grid-refinement study is justified as a continuation of this work, with the optimism that less rather than more dense and complex grids will be required to arrive at useful predictions.

## 7 Acknowledgments

The authors would like to gratefully acknowledge the support of the US Office of Naval Research through the High-Speed Sealift (HSSL) Program. The specific project title was detailed in Section 2.1. The University of Michigan and The University of New South Wales (UNSW) provided infrastructure support.

## 8 References

Ackers, B.B., Michael, T.J., Tredennick, O.W., Landen, H.C., Miller III, E.R., Sodowsky, J.P., and Hadler, J.B.: "An Investigation of the Resistance Characteristics of Powered Trimaran Side-Hull Configurations", *Trans. Society of Naval Architects and Marine Engineers*, Vol. 105, pp 349–368, Discussion: 369–373 (1997)

Armstrong, N.A.: "Coming Soon to a Port Near You: The 126 m Trimaran", *The Naval Architect*, pp 66–78 (September 2004)

Battistin, D., Danielli, A., and Zotti, I.: "Numerical and Experimental Investigations on Wave Resistance of Trimaran Configurations", *Proc. International Maritime Association of Mediterranean IX Congress (IMAM 2000)*, Ischia, Italy, Vol. 1, pp A56–A63 (April 2000)

Begovic, E., Bove, A., Bruzzone, D., Caldarella, S., Cassella, P., Ferrando, M., Tincani, E., and Zotti, I.: "Co-operative Investigation into Resistance of Different Trimaran Hull Forms and Configurations", *Proc. Eighth International Conference on Fast Sea Transportation (FAST '05)*, Saint Petersburg, Russia, 8 pp (June 2005)

Brizzolara, S., Bruzzone, D., and Tincani, E.: "Automatic Optimisation of a Trimaran Hull Form", *Proc. Eighth International Conference on Fast Sea Transportation (FAST '05)*, Saint Petersburg, Russia, 10 pp (June 2005)

Colicchio, G., Colagrossi, A., Lugni, C., and Faltinsen, O.M.: "Experimental and Numerical Investigation of a Trimaran in Calm Water", *Proc. Eighth International Conference on Fast Sea Transportation (FAST '05)*, Saint Petersburg, Russia, 8 pp (June 2005)

Day, A., Clelland, D., Nixon, E.: "Experi-

mental and Numerical Investigation of 'Arrow' Trimarans", *Proc. Seventh International Conference on Fast Sea Transportation (FAST '03)*, Ischia, Italy, Vol. 3, pp D2.23–D2.30 (October 2003)

Degiuli, N., Werner, A., and Doliner, Z.: "Determination of Optimum Position of Outriggers of Trimaran Regarding Minimum Wave Pattern Resistance", *Proc. Seventh International Conference on Fast Sea Transportation (FAST '03)*, Ischia, Italy, Vol. 3, pp D2.15–D2.22 (October 2003)

Degiuli, N., Werner, A., and Zotti, I.: "An Experimental Investigation into the Resistance Components of Trimaran Configurations", *Proc. Eighth International Conference on Fast Sea Transportation (FAST '05)*, Saint Petersburg, Russia, 8 pp (June 2005)

Doctors, L.J.: "On the Great Trimaran-Catamaran Debate", *Proc. Fifth International Conference on Fast Sea Transportation (FAST '99)*, Seattle, Washington, pp 283–296 (August–September 1999)

Doctors, L.J.: "Influence of the Transom-Hollow Length on Wave Resistance", *Proc. Twenty-First International Workshop on Water Waves and Floating Bodies (21 IWWWFB)*, Loughborough, England, 4 pp (April 2006)

Doctors, L.J.: "A Numerical Study of the Resistance of Transom-Stern Monohulls", *Proc. Fifth International Conference on High-Performance Marine Vehicles (HIPER '06)*, Launceston, Tasmania, pp 1–14 (November 2006)

Doctors, L.J. and Beck, R.F.: "The Separation of the Flow past a Transom Stern", *Proc. First International Conference on Marine Research and Transportation (ICMRT '05)*, Ischia, Italy, 14 pp (September 2005)

Doctors, L.J. and Day, A.H.: "Resistance Prediction for Transom-Stern Vessels", *Proc. Fourth International Conference on Fast Sea Transportation (FAST '97)*, Sydney, Australia, Vol. 2, pp 743–750 (July 1997)

Doctors, L.J. and Scrace, R.J.: "The Optimisation of Trimaran Sidehull Position for Minimum Resistance", *Proc. Seventh International Conference on Fast Sea Transportation (FAST '03)*, Ischia, Italy, Vol. 1, pp KL.1–KL.12 (October 2003)

Dubrovsky, V.: *Ships with Outriggers*, Backbone Publishing Company, Fair Lawn, New Jersey, 88+i pp (2004)

Dubrovsky, V. and Lyakhovitsky, A.: *Multi-Hull Ships*, Backbone Publishing Company, Fair Lawn, New Jersey, 495+i pp (2001)

Gale, M.G., Hall, J.H., and Hartley, K.B.: "Trimaran Resistance Experiments — Effect of Outrigger Position", Report DRA/SS/SSHE/CR96015, Defence Research Agency, Farnborough, Hampshire, United Kingdom, 62+xii pp (August 1996)

Gorski, J.: "Evolving Computational Capability for Ship Hydrdynamics", *Naval Surface Warfare Center, Carderock Division, Hydromechanics Department Technical Report,* NSWCCD-50-TR-2004/058 (December 2004)

Kennell, C.: "Model Test Results for a 55 Knot High Speed Sealift Trimaran", *Proc. International Conference on Design and Operation of Trimaran Ships*, Royal Institution of Naval Architects, London, England, pp 195–204 (April 2004)

Lamb, G.R.: "Investigation of a Small-Waterplane-Area Trimaran High-Speed Hullform", *Technical Digest: Technologies for High-Speed Naval Vehicles*, Naval Sea Systems Command, Naval Surface Warfare Center, Carderock Division, Bethesda, Maryland, 44 pp (April 2004)

Leonard, B.P.:"A Stable and Accurate Convective Modeling Procedure Based on Quadratic Upstream Interpolation", *Computer Methods in Applied Mechanics and Engineering*, Vol. 19, pp 59–98 (1979)

Maki, K.J., Doctors, L.J., Beck, R.F., and Troesch, A.W.: "Transom-Stern Flow for High-Speed Craft", *Australian Journal of Mechanical Engineering*, Vol. 3, No. 2, pp 191–199 (2006)

Michell, J.H.: "The Wave Resistance of a Ship", *Philosophical Magazine*, London, Series 5, Vol. 45, pp 106–123 (1898)

Mizine, I., Amromin, E., Crook, L., Day, W., and Korpus, R.: "High-Speed Trimaran Drag: Numerical Analysis and Model Tests", *J. Ship Research*, Vol. 48, No. 3, pp 248–259 (September 2004)

Muzaferija, S., Peric, M., Sames, P., and Schellin, T.: "A Two-Fluid Navier-Stokes Solver to Simulate Water Entry", *Proc. Twenty-Second Symposium on Naval Hydrodynamics*, pp 277–289, Washington, DC (1998)

Narita, S.: "Some Research on the Wave Resistance of a Trimaran", *Proc. International Seminar on Wave Resistance*, Society of Naval Architects of

Japan, Tokyo, Japan, pp 381–388 (February 1976)

Pattison, D.R. and Zhang, J.W.: "Trimaran Ships", *Trans. Royal Institution of Naval Architects*, Vol. 137, pp 143–153, Discussion: 153–161 (1995)

Sasanapuri, B., Shirodkar, V., Wilson, W.M., Kadam, S. and Rhee, S.H.: "Virtual Model Basin for Resistance, Maneuvering, and Seakeeping - a RANS CFD Based Approach", *Twenty-Sixth Int. Conf. Offshore Mech. and Arctic Eng. OMAE '07*, San Diego, California (June 2007)

Scrace, R.J.: "Model Experiments to Investigate the Hydrodynamic Performance of RV Triton", *Proc. International Symposium on RV 'Triton': Trimaran Demonstrator Project*, Royal Institution of Naval Architects, London, England, 10 pp (April 2000)

Summers, A.B. and Eddison, J.F.P.: "Future ASW Frigate Concept Study of a Trimaran Variant", *Proc. International Maritime Defence 1995 Conference*, Spearhead Exhibitions Ltd, London, England, Vol. 1, 59 pp (March 1995)

Suzuki, K. and Ikehata, M.: "Fundamental Study on Optimum Position of Outriggers of Trimaran from View Point of Wave Making Resistance", *Proc. Second International Conference on Fast Sea Transportation (FAST '93)*, Society of Naval Architects of Japan, Yokohama, Japan, Vol. 2, pp 1219–1230 (December 1993)

Wilcox, D. C.: *Turbulence Modeling for CFD*, DCW Industries, Inc., La Canada, California (1998)

Wilson, M.B. and Hsu, C.C.: "Wave Cancellation Multihull Ship Concept", *Proc. High-Performance Marine Vehicle Conference and Exhibit (HPMV '92)*, American Society of Naval Engineers, Washington, pp MH26–MH36 (June 1992)

Wilson, W.M., Fu, T.C., Fullerton, A., and Gorski, J.:"The Measured and Predicted Wave Field of Model 5365: An Evaluation of Current CFD Capability", *Proc. Twenty-Sixth Symposium on Naval Hydrodynamics*, Rome, Italy (September 2006)

Wood, J.E.: "Effect of Increased Outer Hull Setback on Resistance for the O'Neill Hull Form Represented by DTRC Models 5355-1, -2", David Taylor Research Center, Ship Performance Department, Report DTRC/SHD-1147-02, 20+v pp (August 1988)

van Griethuysen, W.J., Bucknall, R.W.G., and Zhang, J.W.: "Trimaran Design — Choices and Variants for Surface Warship Applications", *Future Surface Warships (Warships 2001)*, Royal Institution of Naval Architects, London, England, 19 pp (June 2001)

Yang, C., Noblesse, F., and Löhner, R.: "Practical Hydrodynamic Optimization of a Trimaran", *Trans. Society of Naval Architects and Marine Engineers*, Vol. 109, pp 185–196 (December 2002)

Yang, C., Soto, O., Löhner, R., and Noblesse, F.: "Hydrodynamic Optimization of a Trimaran", *Ship Technology Research: Schiffstechnik*, Vol. 49, No. 2, pp 70–92 (April 2002)

Yasukawa, H.: "Influence of Outrigger Position on the Performances of a High Speed Trimaran (Second Report: Wave-Induced Motions in Head Sea)", *J. Japan Society of Naval Architects and Ocean Engineers*, Vol. 2, pp 189-195 (December 2005)